

Initial Guess Generation for Aircraft Landing Trajectory Optimization

Efstathios Bakolas,^{*} Yiming Zhao[†] and Panagiotis Tsiotras[‡]

School of Aerospace Engineering, Georgia Institute of Technology, Atlanta, GA, 30332-0150

We present a semi-analytic framework for the generation of initial guesses for the numerical solution of the landing trajectory optimization problem of an aircraft. Our approach consists of the following tasks: First, we introduce a geometric framework for the generation of length-suboptimal, curvature-constrained, three-dimensional curves, which satisfy the following requirements: 1) the projection of the curves on the horizontal plane correspond to Dubins-like paths, and 2) an aircraft traveling along these curves is descending continuously until it reaches its final destination. Subsequently, we generate a time-parametrization of the geometric path such that the control inputs required to traverse the geometric path do not exceed the control limits of the aircraft. The resulting time-parameterized path along with the control input time histories is subsequently fed as an initial guess into a numerical optimal control solver, such as the one introduced in Ref. [1]. Simulation results demonstrate the advantages of employing the proposed initial guess generation scheme in terms of convergence of the numerical landing trajectory generation.

Keywords: Landing trajectory generation, numerical trajectory generation, numerical optimal control, three-dimensional Dubins paths.

I. Introduction

We consider the numerical landing trajectory generation problem for a three DOF dynamic model of an aircraft. Typically, when an aircraft operates under normal flight conditions the final stage of the flight (airport approach and landing) is governed by standard/conventional procedures that are enforced and supervised by the air traffic control (ATC). In particular, after the aircraft enters the final approach phase, it is directed by ATC to descend to an intermediate altitude and fly level for miles before proceeding to another lower altitude or joining the final gliding path. This conventional approach is inadequate for emergency landing scenarios for two reasons: First, the landing path of the conventional approach is not optimal in terms of expected arrival time (ETA), which is critical for an emergency landing scenario; moreover, such a path may not even be feasible due to, say, changes over the aircraft dynamics and control authority caused by mechanical failures such as loss of thrust. The second reason has to do with the increased workload of the pilot during an emergency landing scenario. In particular, during a flight emergency, the pilot must perform more tasks than usual in a highly stressful environment; this increases significantly the possibility of flawed decisions and actions. One of the most critical tasks the pilot has to perform is the planning and following of a trajectory that will result in a safe landing. These tasks could be overwhelming to perform and complete in a timely manner.

^{*}Ph.D. candidate, AIAA student member, Email: ebakolas@gatech.edu.

[†]Ph.D. candidate, AIAA student member, Email: yzhao7@gatech.edu.

[‡]Professor, AIAA Fellow, Email: tsiotras@gatech.edu.

To avoid the aforementioned problems that may arise during an emergency landing scenario, it would be helpful to automate the generation of optimal aircraft landing trajectories, that is, without much intervention from the pilots. Numerical optimal control has already been applied to the problem of aircraft trajectory generation. See, for example, Refs. [2–13]. However, not much prior research accounts for the optimal landing problem. A related problem that has been extensively investigated using optimal control theory is the abort landing problem in the presence of wind shear, which has been studied in Refs. [12–14].

Numerical optimal control methods can be classified as direct and indirect methods, both of which require a set of initial guesses to start the optimization process. It is also well known that a good initial guess is helpful for the convergence of both methods. Direct approaches usually have a larger domain of convergence, hence they are relatively more robust than indirect methods. For this reason they have been used to generate initial guesses for indirect methods when highly accurate solutions are required.^{15–17} However, for a complicated problem, like the landing trajectory generation for a fixed-wing aircraft, convergence could be problematic even when using a direct methods, in which case a good initial guess would be highly desirable.

An initial guess for a direct method includes the time history of all state and control variables as well as any unknown parameters. In order for an initial guess to be dynamically feasible, it is necessary that all state and control time histories satisfy the equations of motion, as well as the control and state constraints, rendering the generation of a dynamically feasible initial guess not an easy task.

In this work, we introduce a simple scheme for the generation of an initial guess for the numerical optimal control solver DENMRA, introduced in Ref. [1]. The generation of the initial guess is based on the suboptimal solution of a three-dimensional variation of the classical Markov–Dubins problem,¹⁸ that is, the problem of characterizing curvature-constrained paths of minimum length in the plane. It is shown that this approach, although fairly simple, can effectively improve the convergence of the numerical optimal control solver for the minimum time landing trajectory optimization problem.

We propose a semi-analytic framework for the generation of a set of initial guesses for the numerical landing trajectory optimization problem, which consists of two parts. First, we generate a geometric path which connects the initial and terminal configurations of the aircraft satisfying the following requirements: (1) the projection of the three-dimensional curve onto the horizontal plane corresponds to a Dubins-like path, that is, a composite path that solves the Markov–Dubins problem.¹⁸ A solution of the Markov–Dubins problem is formed, in turn, by concatenations of circular arcs and line segments; and (2) an aircraft traveling along this path is continuously descending until it reaches its final destination. Note that a geometric path that satisfies simultaneously the previous two requirements may not necessarily be a solution of either the three-dimensional version of the Markov–Dubins problem,¹⁹ nor a minimum-time trajectory of the Dubins airplane.²⁰ Using standard techniques from the optimal synthesis of the Markov–Dubins problem,^{21–23} we show that a family of path primitives that consists of circular arcs, line segments and helical arcs is sufficiently rich for generating composite paths that satisfy the previous geometric requirements for arbitrary boundary conditions. Second, we generate a time-optimal speed profile along the geometric path that captures succinctly the motion constraints of the aircraft while ensuring minimum time travel along the path. Subsequently, we compute the time histories of the control inputs required so that the aircraft can traverse the geometric path with the assigned speed profile using inverse dynamics.²⁴ We thus obtain a feasible trajectory along with the corresponding control inputs histories, which can be subsequently used as an initial guess for the numerical optimization of the landing trajectory.

The rest of the paper is organized as follows. In Sections II–III, we present a scheme for the construction of a three-dimensional curvature constrained path. In Section IV, we discuss the problem of assigning a time-optimal speed profile along this geometric path; this allows us to

compute the control input histories through inverse dynamics. In Section V, we demonstrate how the time parameterized curve along with the time histories of the corresponding control inputs, which were characterized in Sections II–IV, can serve as an initial guess for the numerical solution of the landing trajectory optimization problem. Simulation results are presented in Section VI. Finally, Section VII concludes the paper with a summary of remarks.

II. Three-dimensional Landing Path Generation

In this section, we present an analytical framework for the generation of curvature constrained paths in three dimensions. The paths are solutions of a steering problem for a particle of unit mass that travels in a three-dimensional Euclidean space. Each path is generated by appropriate concatenations of the elements of a sufficiently rich family of path primitives.

II.A. Kinematic Model and Problem Formulation

First, we consider the problem of characterizing geometric paths of minimal length connecting two points in the three-dimensional space with prescribed tangents. The geometric problem can be formulated equivalently as an optimal control problem of a particle of unit mass. In particular, the kinematic model we employ is described by the following set of equations

$$x' = \cos \psi \cos \gamma, \quad (1)$$

$$y' = \sin \psi \cos \gamma, \quad (2)$$

$$z' = \sin \gamma, \quad (3)$$

$$\psi' = \frac{u}{R_{\min}(z)}, \quad (4)$$

where $(x, y, z) \in \mathbb{R}^3$ is the position vector, $\psi \in [0, 2\pi)$ is the velocity heading of the particle, $R_{\min}(z)$ is a positive quantity, which may depend on the altitude z , γ is the flight path angle (control input), and u is the second control input that determines the rate of change of the heading angle. The prime denotes differentiation with respect to the arc length s . It is assumed, furthermore, that $\gamma \in [\gamma_{\min}, \gamma_{\max}] \subseteq [-\pi/2, \pi/2]$, and $u \in [-\delta, 1]$, where $\delta \in (0, 1]$ (i.e., the steering constraints may be asymmetric²⁵).

II.B. The Minimum-Length Problem

Next, we formulate the minimum-length problem as an optimal control problem.

Problem 1 *Find the controls u^* and γ^* that steer the system described by Eqs.(1)-(4) from (x_0, y_0, z_0, ψ_0) (prescribed) to (x_f, y_f, z_f, ψ_f) (prescribed) such that the total length of the ensuing path s_f (free) is minimum.*

The kinematic model described by Eqs. (1)-(4) for the special case when $R_{\min}(z) = \bar{R}$, where \bar{R} is a positive constant, for all $z \geq 0$, was introduced by Chitaz and Lavelle in Ref. [20]. The authors of Ref. [20] have shown that the minimum-length paths of this special case of Problem 1 are necessarily concatenations of the following path primitives: (1) circular arcs of turning radius \bar{R} and path angle $\gamma = 0$; (2) straight line segments, and (3) arcs of helical paths of radius \bar{R} and a path angle $\gamma \in \{\gamma_{\min}, \gamma_{\max}\}$. The authors of Ref. [20] only discuss the structure of the optimal paths for the special case of Problem 1 when $R_{\min}(z) = \bar{R}$, without touching upon the more challenging and practical problem of determining the minimum-length paths for a given pair of prescribed initial and terminal configurations (i.e., the *synthesis* problem). The difficulty of the synthesis problem stems from the large number of candidate optimal paths that arise when taking arbitrary concatenations of the path primitives.²⁰ As part of this work, we are interested in addressing the problem of synthesis of suboptimal solutions of the following variation of Problem 1.

Problem 2 Solve Problem 1, when $z(s) > z_f$, for all $s \geq 0$, and $\gamma_{\max} = 0$.

Note that besides the continuous descent requirement ($\gamma \leq 0$), the formulation of Problem 2 does not constraint the landing paths to satisfy a constant minimum turning radius constraint during the whole landing phase, in contrast to the problem formulation of Ref. [20].

III. Suboptimal Synthesis of the Three-Dimensional Path Planning Problem

In this section, we investigate the problem of characterizing a nearly minimum-length path that solves Problem 2 for any prescribed pair of boundary configurations. A straightforward way to characterize suboptimal solutions of Problem 2 is to decouple the path planning problem into a steering problem in the x - y plane (or more precisely $\mathbb{R}^2 \times \mathbb{S}^1$), and another steering problem in the vertical plane (one-dimensional problem).

III.A. The Minimal Length Curve Problem in the Horizontal Plane

First, we address a path planning problem in the horizontal plane x - y , which will allow us to address the three-dimensional path planning problem (Problem 2). To this aim, we assume that the solution of the steering problem in $\mathbb{R}^2 \times \mathbb{S}^1$ follows the Dubins pattern, that is, the projection of a (suboptimal) solution of Problem 2 on the x - y plane is a concatenation of two circular arcs of minimum radius interconnected by either a straight line or another circular arc as shown in Fig 1. Note that the radii of the circular arcs of the projection of a path that solves Problem 2 on the x - y plane need not be equal as a result of the fact that the steering capacity of the aircraft depends on the altitude.

In order to obtain a simple formula for computing the minimum turning radius of an aircraft as a function of the altitude, we first observe that the rate of change of ψ of an aircraft of mass m traveling with speed v at an altitude z is given by²⁶

$$\psi' = -\frac{L(C_L, v, z) \sin \phi}{mv^2 \cos \gamma}, \quad (5)$$

where ϕ is the bank angle, $L = L(C_L, v, z)$ is the lift and C_L is the lift coefficient. If we assume that $v = v(z)$, we can obtain a rough approximation of R_{\min} as follows

$$R_{\min}(z; \gamma) = \frac{mv^2(z) \cos \gamma}{L(C_L^{\max}, v(z), z) \sin \phi_{\max}}, \quad (6)$$

where ϕ_{\max} and C_L^{\max} denote, respectively, the upper bounds on the bank angle and the lift coefficient. Equation (6) implies that an aircraft is less maneuverable, in terms of performing sharp turns, at higher altitudes than it is at lower altitudes. Let $R_0 \triangleq R_{\min}(z_0; 0)$, $R_f \triangleq R_{\min}(z_f; 0)$ and $R_m \triangleq R_{\min}(z_m; 0)$, where $z_m = (z_0 + z_f)/2$. In addition, let us assume that along the first and the last circular arcs of the Dubins path the quantity R_{\min} in Eq.(4) is constant and equal to R_0 and R_f , respectively. Furthermore, if the Dubins path consists of three circular arcs, then the quantity R_{\min} along the middle arc is constant and equal to R_m . Note that $R_0 \geq R_m \geq R_f$. In order to obtain more conservative estimates of the R_{\min} , and thus reduce the risk of selecting a small value for the minimum turning radius that can lead to dynamically infeasible paths for the aircraft, we multiply R_0 , R_m , and R_f by a safety factor k_0 , k_m , and $k_f > 1$, respectively.

Next, we formulate a minimum-length problem on the horizontal plane (x - y plane).

Problem 3 Given two configurations (x_0, y_0, ψ_0) and (x_f, y_f, ψ_f) in $\mathbb{R}^2 \times \mathbb{S}^1$, find a minimum-length curve that connects the two configurations and belongs necessarily to the following family of paths

$$\mathcal{P} \triangleq \{C^\pm(R_0) \circ C^\mp(R_m) \circ C^\pm(R_f), C^\pm(R_0) \circ S \circ C^\pm(R_f), C^\pm(R_0) \circ S \circ C^\mp(R_f)\}, \quad (7)$$

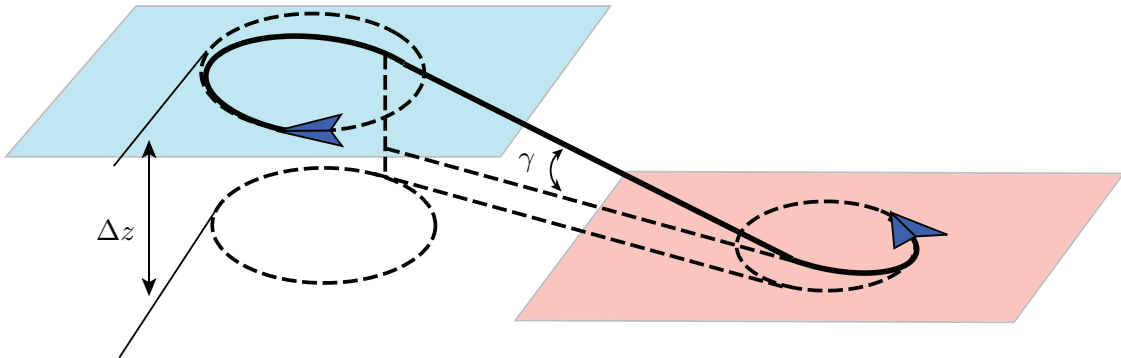
where $C^-(R_\ell)$ ($C^+(R_\ell)$) and S denote a circular arc of radius R_ℓ , where $\ell \in \{0, m, f\}$, traversed clockwise (counterclockwise) and a line segment, respectively, and \circ denotes the concatenation of two consecutive arcs of the composite path.

III.B. The Minimal Length Curve Problem in the Vertical Plane

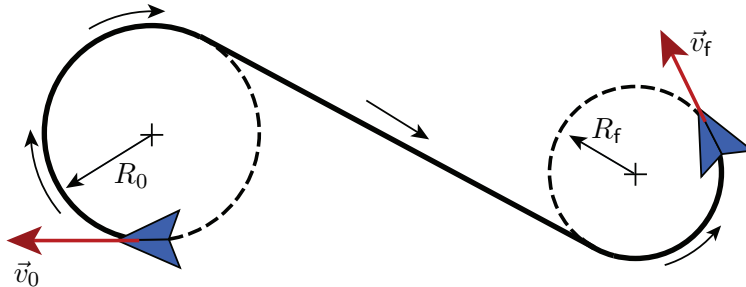
Next, we address the steering problem in the vertical plane. The solution of the latter problem, along with the solution of the previously discussed steering problem in the horizontal plane, will allow us to characterize the (suboptimal) solutions for Problem 2.

In our subsequent analysis, we limit our attention to paths of piecewise constant path angle. In particular, we assume that, along an arc whose projection on the x - y plane is an arc of a Dubins path, the path angle γ is constant. Thus $\gamma \in \{\gamma_0, \gamma_m, \gamma_f\}$, where $\gamma_i \in [\gamma_{\min}, 0]$, $i \in \{0, m, f\}$. Note that, ideally, one would choose $\gamma = \gamma_{\min}$ along the whole path, since this choice would maximize the vertical (downward) component of the velocity vector (and thus minimize the length of the descent path). As we shall see shortly afterwards, this approach may not always furnish feasible solutions to Problem 2. Before proceeding to a more detailed treatment of Problem 2, we will introduce some new notation. Specifically, we denote by $s_1 \leq s_2 \leq s_3$ the arc length of the ensuing path of the vehicle when the latter reaches the endpoint of, respectively, the first, the second and the third arc of the Dubins path, which is the projection of the solution of Problem 2 on the x - y plane. We will always assume that $s_0 = 0$. Note that, in general, $s_f \neq s_3$ for reasons we shall explain later on. Next, we denote by $z_1 \geq z_2 \geq z_3$ the altitude of the aircraft at $s = s_1$, $s = s_2$ and $s = s_3$, when $\gamma = \gamma_{\min}$. Specifically,

$$z_1 = z_0 + s_1 \sin \gamma_{\min}, \quad z_2 = z_1 + (s_2 - s_1) \sin \gamma_{\min}, \quad z_3 = z_2 + (s_3 - s_2) \sin \gamma_{\min}. \quad (8)$$



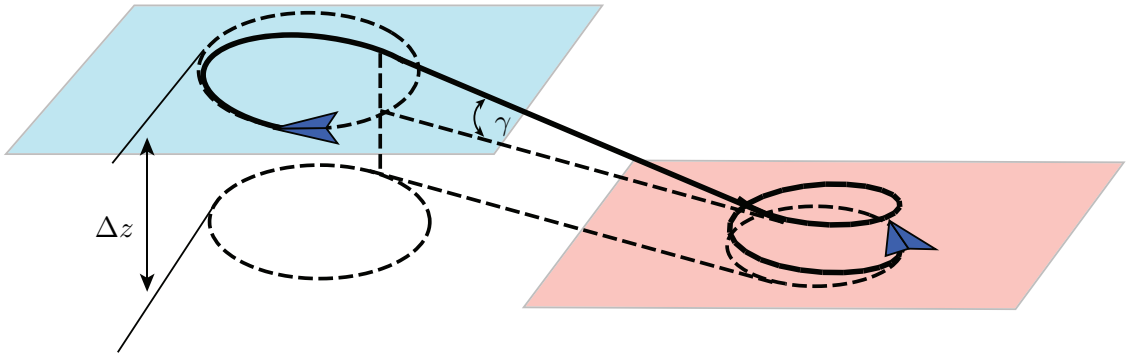
(a) The 3D view of the landing path.



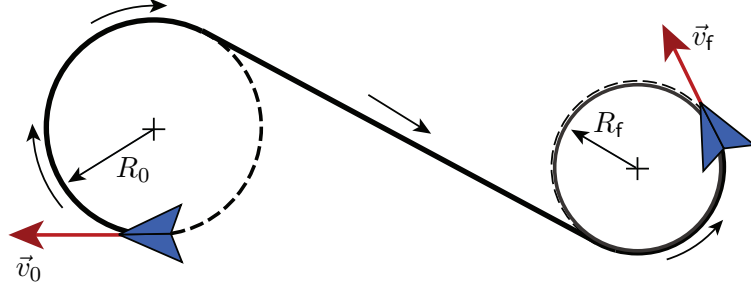
(b) The projection of the landing path onto the x - y plane.

Figure 1. A simple scheme for generating three-dimensional paths whose projections on the x - y plane are Dubins paths.

Next, we examine the following four cases:



(a) The 3D view of the path.



(b) Projection of the landing path onto the $x - y$ plane.

Figure 2. If the aircraft cannot decrease enough its altitude along the first two arcs of the composite path, then it may have to perform one or more loops along the last helical arc of the path.

Case I: $z_1 \leq z_f$. If $z_1 = z_f$, then $\gamma_0 = \gamma_{\min}$ and $\gamma_m = \gamma_f = 0$, that is, the last two arcs of the path correspond to steady and level flight at altitude $z = z_f$, and, furthermore, $s_f = s_3$. If $z_1 < z_f$, then we set the path angle along the first arc to be the solution $\gamma_0^* > \gamma_{\min}$ of the following equation

$$z_f = z_0 + s_1 \sin \gamma_0^*. \quad (9)$$

Note that $s_1 = s_1(\gamma_0^*)$ and $s_f = s_3$. In addition, since for $\gamma = \gamma_0^*$, $z(s_1) = z_f$, it follows that $\gamma_m = \gamma_f = 0$. The situation is illustrated in Fig. 3(a).

Case II: $z_1 > z_f$ and $z_2 \leq z_f$. If $z_2 = z_f$, then necessarily $\gamma_f = 0$, and the last arc of the path corresponds to a steady level turns at $z = z_f$. If $z_2 < z_f$, then we set the path angle along the second arc to be the solution γ_m^* of the following equation

$$z_f = z_1 + (s_2 - s_1) \sin \gamma_m^*. \quad (10)$$

Note that $s_2 = s_2(\gamma_m^*)$. It follows as in Case I that $\gamma_f = 0$ and $s_f = s_3$. The situation is illustrated in Fig. 3(b).

Case III: $z_1 > z_f$, $z_2 > z_f$ and $z_3 \leq z_f$. In this case, $\gamma_0 = \gamma_m = \gamma_{\min}$. If $z_3 = z_f$, then $\gamma_f = \gamma_{\min}$ as well. If $z_3 < z_f$, then γ is taken to be the solution $\gamma_f^* > \gamma_{\min}$ of the following equation

$$z_f = z_2 + (s_3 - s_2) \sin \gamma_f^*. \quad (11)$$

Note that $s_3 = s_3(\gamma_f^*)$ and $s_f = s_3$. The situation is depicted in Fig. 3(c).

Case IV: $z_3 > z_f$. In this case, the downward velocity is not sufficiently large to guarantee that an aircraft traversing a path whose projection on the $x-y$ plane is a Dubins path can reach the desired final altitude at the end of its course. In order to increase the length of the descent path without changing the structure of the Dubins path in the $x-y$ plane, we can add one or more

loops along the last helical arc. In this way, the projection of the last arc on the x - y plane will remain the same but the length of the ensuing path will be increased. In particular, if $s_{\text{loop}}(\gamma)$ is the total length of a full loop at constant path angle γ , we wish to find the minimum path angle $\gamma_f^* \in (\gamma_{\min}, 0)$, and the minimum number of loops $n_{\text{loop}} \in \{1, 2, \dots\}$ such that

$$z_f = z_2 + (s_3 + n_{\text{loop}}s_{\text{loop}} - s_2) \sin \gamma_f^*. \quad (12)$$

Note that in this case $s_f \neq s_3$. In addition, s_f satisfies the following equation

$$s_f = s_3 + n_{\text{loop}}s_{\text{loop}}. \quad (13)$$

The situation is illustrated in Fig. 3(d).

III.C. A Family of Path Primitives for the Three-Dimensional Path Planning Problem

By combining the solutions of the path planning problems on the horizontal and the vertical planes, we characterize a family of path primitives that, when combined appropriately, furnish near-optimal solutions of Problem 2. The family of path primitives we propose to use in order to generate suboptimal solutions of Problem 2 is given by

$$\begin{aligned} \mathcal{P}_{3D} \triangleq & \{H^\pm(R_0, \gamma_0^*) \circ H^\mp(R_m, 0) \circ H^\pm(R_f, 0), H^\pm(R_0, \gamma_{\min}) \circ H^\mp(R_m, \gamma_m^*) \circ H^\pm(R_f, 0), \\ & H^\pm(R_0, \gamma_{\min}) \circ H^\mp(R_m, \gamma_{\min}) \circ H^\pm(R_f, \gamma_f^*), H^\pm(R_0, \gamma_{\min}) \circ H^\mp(R_m, \gamma_{\min}) \circ H^\pm(R_f, \gamma_{\min}), \\ & H^\pm(R_0, \gamma_0^*) \circ S \circ H^\pm(R_f, 0), H^\pm(R_0, \gamma_{\min}) \circ S \circ H^\pm(R_f, 0), H^\pm(R_0, \gamma_{\min}) \circ S \circ H^\pm(R_f, \gamma_f^*), \\ & H^\pm(R_0, \gamma_{\min}) \circ S \circ H^\pm(R_f, \gamma_{\min}), H^\pm(R_0, \gamma_0^*) \circ S \circ H^\mp(R_f, 0), H^\pm(R_0, \gamma_{\min}) \circ S \circ H^\mp(R_f, 0), \\ & H^\pm(R_0, \gamma_{\min}) \circ S \circ H^\mp(R_f, \gamma_f^*), H^\pm(R_0, \gamma_{\min}) \circ S \circ H^\mp(R_f, \gamma_{\min})\}, \end{aligned}$$

where $H^-(R, \gamma)$ ($H^+(R, \gamma)$) denote a helical arc of radius R and path angle γ traversed clockwise (counterclockwise) when observed from above, where $R \in \{R_0, R_m, R_f\}$ and $\gamma \in \{0, \gamma_0^*, \gamma_m^*, \gamma_f^*\}$, and S denotes a line segment.

IV. Minimum-Time Landing Trajectory Initial Guess Generation

In the previous section, we introduced a method for generating a geometric landing path using a simplified aircraft model. The generated landing path, however, does not contain time information, hence it cannot function as an initial guess for a numerical optimal control scheme. In order to be able to use this geometric path as a reliable initial guess, we need to assign a time parametrization along the path using an aircraft model that captures the aircraft dynamics more accurately. In this way, the initial geometric path is combined with a time history of all state and control variables of a high fidelity aircraft model, which are subsequently used as part of the initial guess for the landing trajectory optimization problem.

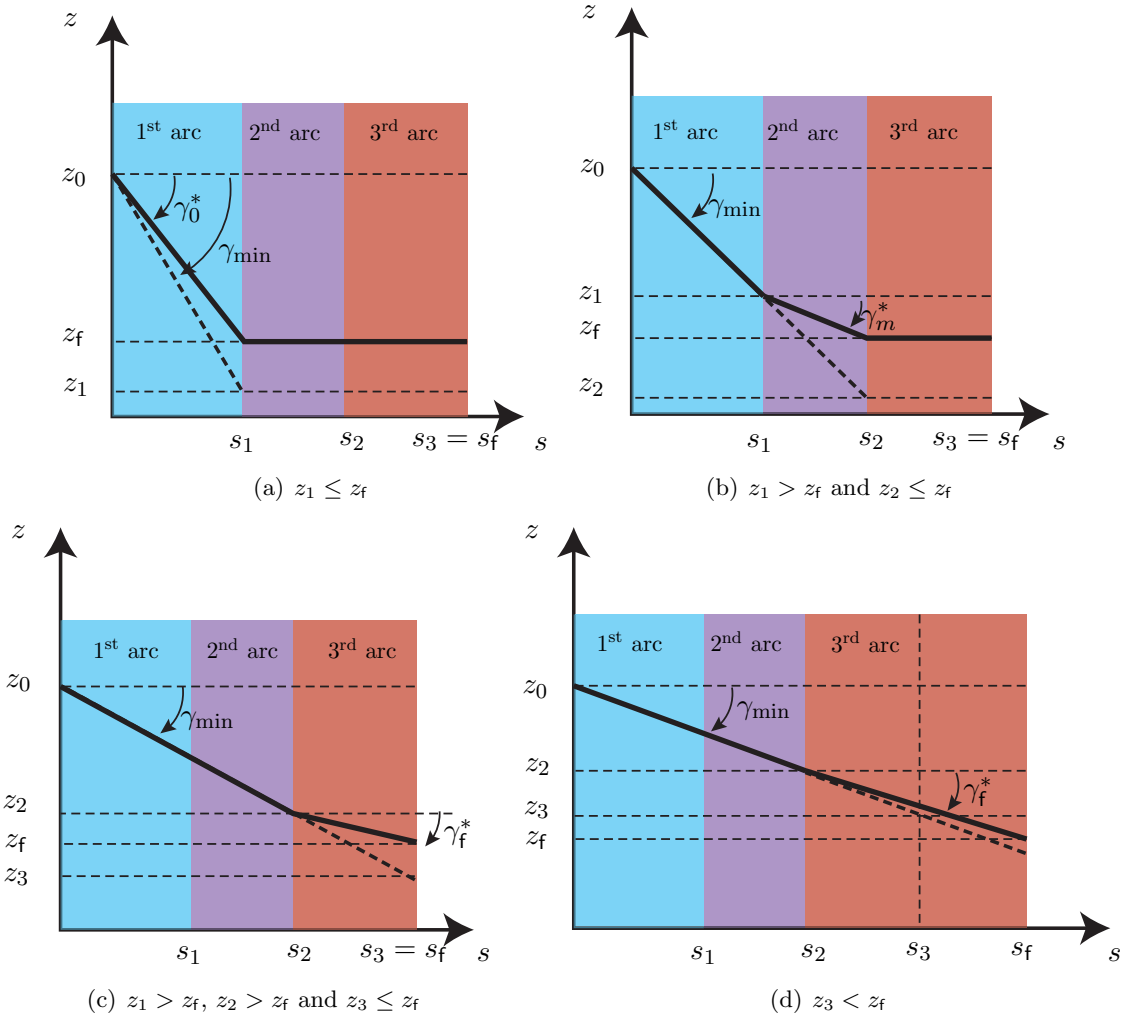


Figure 3. The path angle γ v/s arc length s profile.

IV.A. Aircraft Model

We consider the following aircraft model for trajectory optimization, with kinematic and dynamical equations given below:²⁶

$$\dot{x} = v \cos \gamma \cos \psi, \quad (14)$$

$$\dot{y} = v \cos \gamma \sin \psi, \quad (15)$$

$$\dot{z} = v \sin \gamma, \quad (16)$$

$$\dot{v} = \frac{1}{m} [T - D(C_L, v, z) - mg \sin \gamma], \quad (17)$$

$$\dot{\gamma} = \frac{1}{mv} [L(C_L, v, z) \cos \phi - mg \cos \gamma], \quad (18)$$

$$\dot{\psi} = -\frac{L(C_L, v, z) \sin \phi}{mv \cos \gamma}, \quad (19)$$

where v is the speed, $\rho_{\text{air}}(z)$ is the air density at altitude z , ϕ is the bank angle, and x, y, z and ψ are the same as in (1)-(4). The aerodynamic lift force $L(C_L, v, \rho_{\text{air}})$ and drag force $D(C_L, v, \rho_{\text{air}})$ are given by:

$$\begin{aligned} L(C_L, v, z) &= \frac{1}{2} \rho_{\text{air}}(z) v^2 S_w C_L, \\ D(C_L, v, z) &= \frac{1}{2} \rho_{\text{air}}(z) v^2 S_w C_D = \frac{1}{2} \rho_{\text{air}}(z) v^2 S_w (C_{D_0} + K C_L^2), \end{aligned}$$

where C_{D_0} and K are constants determined by the aerodynamic properties of the aircraft, and S_w is the main wing surface area. The control inputs in this model include the lift coefficient C_L , the bank angle ϕ , and the thrust T . The effect of the wind is not considered in this model. Because the total time of a landing process is relatively short, the mass of the aircraft m is assumed to be constant. In order to account for the air density change during the landing process, we adopt the atmospheric model presented in Ref. [27]. The parameters in the model are listed in Table 1, where T_{max} denotes the maximum thrust.

Table 1. Aircraft model and relevant data.

m	g	S_w	C_{D_0}	K	T_{max}
288,938 kg	9.8 kgm/s ²	510.97 m ²	0.022	0.045	1126.3 kN

IV.B. Time Parametrization and Inverse Dynamics

In this section, we present a scheme for assigning a speed profile, or equivalently, attaching a time parametrization, to the geometric path characterized using the approach of Sections II–III. The difficulty of the speed profile assignment problem has to do with the fact that the assignment has to be made in a way such that the resulting trajectory (time parameterized path) is a *feasible* landing trajectory for the dynamical model described by Eq. (14)–(19), that is, there exist controls with which the aircraft can follow the path without violating any control and speed constraints.

The time-optimal parametrization method introduced in Ref. [24] is applied for tuning the parameters including k_0 , k_f , and γ_{min} , which are used in the geometric path planning method introduced in Sections II–III. This time-optimal parameterization method is also applied for generating a minimum-time trajectory initial guess for a numerical optimal control algorithm as discussed in Section V.

Because the given path is naturally parameterized using the path coordinate s instead of time, a geometric path can be described by $(x(s), y(s), z(s)) \in \mathbb{R}^3$, $s \in [s_0, s_f]$. The equations of motion can be rewritten with respect to s as follows (where prime denotes differentiation with respect to s):

$$x' = \cos \gamma \cos \psi, \quad (20)$$

$$y' = \cos \gamma \sin \psi, \quad (21)$$

$$z' = \sin \gamma, \quad (22)$$

$$v' = \frac{1}{mv} [T - D(C_L, v) - mg \sin \gamma], \quad (23)$$

$$\gamma' = \frac{1}{mv^2} [L(C_L, v) \cos \phi - mg \cos \gamma], \quad (24)$$

$$\psi' = -\frac{L(C_L, v, z) \sin \phi}{mv^2 \cos \gamma}. \quad (25)$$

The following relations have been used for deriving (20)-(25):

$$dt = \frac{ds}{v}, \quad (26)$$

$$ds = \sqrt{dx^2 + dy^2 + dz^2}, \quad (27)$$

$$\psi = \arctan \frac{dy}{dx} = \arctan \frac{y'}{x'}, \quad (28)$$

$$\gamma = \arctan \frac{dz}{\sqrt{dx^2 + dy^2}} = \arctan \frac{z'}{\sqrt{x'^2 + y'^2}}, \quad (29)$$

$$\psi' = \frac{1}{1 + (y'/x')^2} \frac{y''x' - y'x''}{x'^2} = \frac{x'^2}{x'^2 + y'^2} \frac{y''x' - y'x''}{x'^2} = \frac{y''x' - y'x''}{x'^2 + y'^2}, \quad (30)$$

$$\gamma' = \frac{z''x'^2 + z'y'^2 - z'x''x' - z'y''y'}{\sqrt{x'^2 + y'^2}}. \quad (31)$$

The initial guess comprising of both state and control histories along with the previously proposed geometric path is obtained by solving the following problem which is considered in Ref. [24]:

Problem 4 (Minimum-time path following) *Given a geometric path $(x(s), y(s), z(s))$, where $s \in [s_0, s_f]$ is the path coordinate, and the aircraft dynamics as described by Eq. (20)–(25), find the optimal control time history $C_L^*(t)$, $\phi^*(t)$, $T^*(t)$ such that the aircraft follows the path in minimum time without violating any state/control constraints or boundary conditions.*

It has been shown in Ref. [24] that Eq. (20)–(25) form algebraic constraints on the state variables for Problem 4. While Eq. (20)–(22) are automatically satisfied due to the geometric relation between the path and the states variables ψ and γ , the control bounds on the lift coefficient C_L and bank angle ϕ can be converted into simple bounds on the speed v through Eq. (24) and (25). Letting, for notational simplicity, $E = v^2/2$, then Problem 4 is equivalent to the following *one-dimensional* optimization problem:

$$\begin{aligned} \min_T \quad & J(s_0, s_f, E(s_0), E(s_f), T) = t_f = \int_{s_0}^{s_f} \frac{ds}{\sqrt{2E(s)}}, \\ \text{subject to} \quad & E'(s) = \frac{T(s)}{m} + c_1(s)E(s) + \frac{c_2(s)}{E(s)} + c_3(s), \\ & \underline{g}_w(s) \leq E(s) \leq \bar{g}_w(s), \quad s \in [s_0, s_f] \\ & E(s_0) = v_0^2/2, \quad E(s_f) = v_f^2/2, \\ & T_{\min} \leq T(s) \leq T_{\max}, \quad s \in [s_0, s_f] \end{aligned} \quad (32)$$

where v_0 and v_f are the required initial and final speed at s_0 and s_f , respectively. The functions \bar{g}_w and \underline{g}_w describe the constraints on E as determined by Eq. (24) and (25). For details regarding the explicit derivation of \bar{g}_w and \underline{g}_w , the reader can refer to Ref. [24]. The functions c_1 , c_2 and c_3 are determined by the path as follows.²⁴

$$c_1(s) \triangleq -\frac{C_{D_0}(s)\rho_{\text{air}}(s)S_w}{m} - \frac{4Km\gamma'^2(s)}{\rho_{\text{air}}(s)S_w} - \frac{2Km\cos^2\gamma(s)\psi'^2(s)}{\rho_{\text{air}}(s)S_w}, \quad (33)$$

$$c_2(s) \triangleq -\frac{Kmg^2\cos^2\gamma(s)}{\rho_{\text{air}}(s)S_w}, \quad (34)$$

$$c_3(s) \triangleq -\frac{4Km\gamma'(s)g\cos\gamma(s)}{\rho_{\text{air}}(s)S_w} - g\sin\gamma(s). \quad (35)$$

Once a geometric path is generated using the method introduced in Sections II–III, then the minimum-time parametrization is solved using the algorithm presented in [24], which yields the optimal speed profile solving Problem 4. Subsequently, the optimal thrust T^* can be computed from Equation (32). The other control inputs are generated using inverse dynamics as follows:

$$C_L^*(s) = \frac{2}{\rho_{\text{air}}v^{*2}(s)S_w} \left(T^*(s) - mv^*(s)v^{*'}(s) - mg\sin\gamma(s) \right),$$

$$\phi^*(s) = -\arctan \left(\frac{\cos\gamma(s)\psi'(s)}{\gamma'(s) + g\cos\gamma(s)/v^{*2}(s)} \right).$$

Before proceeding to the complete solution to the optimal landing problem, the previous time parametrization method is also used to tune key parameters in the geometric path planning process, since a well-tuned geometric path will generate better initial guesses, thus helping with the convergence of the numerical optimization solver. For the aircraft model used in this paper, it was found that the generated paths are mostly feasible with $k_0 = 5$, $k_f = 2$, and $\gamma_{\min} = -7$ deg. When the generated geometric path is not feasible, free initial and final speed conditions are applied to Problem 4 to generate a trajectory.

V. Landing Trajectory Optimization Using Numerical Optimal Control

It is important to note that the time-optimal parametrization method presented in the previous section only provides a feasible trajectory, whose time optimality holds only when the aircraft is constrained to travel along the specified path. In addition, the path itself, which is generated based on the simplified aircraft model and certain heuristic methods presented in Sections II–III, is not, in general, a time-optimal path of the higher fidelity aircraft model. Consequently, the corresponding initial landing trajectory is not optimal as well.

In order to further improve the time optimality of the landing trajectory while ensuring its feasibility, we formulate the emergency landing problem as a minimum-time optimal control problem, and then apply a direct method to obtain an optimal solution by solving a relevant nonlinear programming problem, utilizing the initial trajectory generation techniques introduced in Sections II–III and IV. In the following, we briefly discuss about the nonlinear programming formulation of the optimal control problem and the numerical optimization procedure to which the three-dimensional landing trajectory initial guess is applied.

The minimum-time landing problem considered in this paper minimizes the total flight time t_f while satisfying the following three different types of constraints:

1. The differential dynamic constraints (14)-(19). For notational convenience, let $X : \mathbb{R} \rightarrow \mathbb{R}^6$

be the vector-valued function such that

$$X(t) = [x(t), y(t), z(t), v(t), \gamma(t), \psi(t)]^T.$$

Similarly, define $U : \mathbb{R} \rightarrow \mathbb{R}^3$ by

$$U(t) = [C_L(t), \phi(t), T(t)]^T,$$

and let $f : \mathbb{R}^6 \times \mathbb{R}^3 \rightarrow \mathbb{R}^6$ be the vector valued-function representing the right-hand-side of the differential equations (14)-(19). Then the dynamic constraints can be written compactly as

$$\dot{X} = f(X, U). \quad (36)$$

2. The state and control constraints. To be more consistent with the actual physics of the aircraft, we impose bounds on the control variables. We also consider limits on the speed v and the flight path angle γ for flight envelope protection. These state and control bounds are given below:

$$\begin{aligned} C_L(t) &\in [-0.27, 1.73], & \phi(t) &\in [-30, 30] \text{ deg}, & T(t) &\in [0, T_{\max}], \\ v(t) &\in [80, 270] \text{ m/s}, & \gamma(t) &\in [-20, 0] \text{ deg}. \end{aligned}$$

Similar to (36), a function $C : \mathbb{R}^6 \times \mathbb{R}^3 \rightarrow \mathbb{R}^{10}$ is defined such that the state and control bounds can be expressed by

$$C(X, U) \leq 0. \quad (37)$$

3. The boundary conditions. The states of the aircraft (position, speed, heading and flight path angle) are fixed at the very beginning and the end of the flight, therefore we consider the following boundary conditions:

$$X(t_0) = X_0, \quad X(t_f) = X_f.$$

These constraints are simply written as

$$\Psi(X(t_0), X(t_f)) = 0, \quad (38)$$

where the domain and image of the function Ψ have appropriate dimensions.

With these three types of constraints, the minimum-time landing problem can formulated as follows:

Problem 5 (Optimal control formulation of the aircraft minimum-time landing problem)

$$\begin{aligned} \min_U \quad & t_f \\ \text{subject to} \quad & \dot{X}(t) = f(X(t), U(t)), \\ & C(X(t), U(t)) \leq 0, \quad t \in [t_0, t_f], \\ & \Psi(X(t_0), X(t_f)) = 0. \end{aligned}$$

To solve this optimal control problem using nonlinear programming, the states and controls are discretized on a mesh $\{t_i\}_{i=0}^N$ containing N grid points, with $t_N = t_f$ and $t_i < t_{i+1}$ for $0 \leq i \leq N-1$. The discretized state and control variables plus the final time t_f are the decision variables in the NLP problem. The differential constraints are discretized and converted to finite difference equations using a certain discretization scheme.^{1,28} The finite difference equations are enforced

as algebraic constraints on the decision variables. The other constraints, including the state and control constraints, etc., are enforced at each grid point also as algebraic constraints. The reader may refer to Ref. [28] for more details about discretizations of optimal control problems.

The mesh refinement algorithm DENMRA¹ is used to convert Problem 5 into an NLP using the trapezoidal integration rule. DENMRA uses density functions to determine the local distribution of grid points. The trapezoidal rule is chosen to balance the convergence speed and accuracy while ensuring the consistency of approximation.

The resultant NLP is solved using the sparse nonlinear optimization software SNOPT.²⁹ The three-dimensional landing trajectory introduced in Section IV is used as an initial guess to start SNOPT.

It is well-known that the convergence of any NLP solver strongly depends on the quality of the initial guess—with a good initial guess, the NLP solver is much more likely to converge. The geometric path generated as in Section II–III is a ‘reasonably good’ landing path. Besides, the feasibility of the trajectory along the path is ensured by the time-optimal parametrization technique in Section IV (if such a parametrization exists, it renders the path feasible). Therefore, the initial landing trajectory is usually feasible and close to the optimal solution, thus facilitating convergence of the numerical scheme.

VI. Numerical Simulations

In this section, we present the numerical results obtained by applying the initial guess generation approach presented in the previous sections to the landing trajectory optimization problem. In all numerical experiments, DENMRA starts from a uniform mesh containing 25 grid points and ends up with 40 grid points after three mesh refinements and a total of four rounds of optimization. The geometric landing path generated as in Sections II–III is processed using the time parametrization method to obtain the initial guess for starting the first round of optimization in DENMRA. After the optimization result is obtained, it is used for mesh refinement as well as an initial guess to start the next round of optimization. The final optimization result is considered feasible if the maximum local integration error between each adjacent pair of grid points is smaller than 10^{-5} .

The numerical results showed that the initial landing trajectory generated using the method presented in Sections II–III and IV usually captures the key features of a locally optimal solution, as it is illustrated in Figs. 4 and 5. In these plots, the red lines denote the initial guess paths, and the blue lines with markers are the paths which correspond to the optimization results of DENMRA. A difference between the initial guess and the final optimal trajectory is observed for some cases, in particular, when the horizontal range of flight (horizontal distance between the aircraft’s initial position and the airport) is small, as shown in Fig. 6. Simulation results indicate that the geometry of the optimal landing trajectory is related to the ratio of the horizontal range to the altitude change. When this ratio is large enough, the flight time is mainly determined by the aircraft’s movement in the horizontal plane, and the projection of the optimal trajectory to the horizontal plane resembles the typical circle-straight line-circle pattern of the Dubins’ path for shorter travel time. When this ratio is small, the total flight time is primarily limited by the aircraft’s descent dynamics—the aircraft must fly over certain horizontal distance to lose altitude, in which case the optimal landing trajectory tend to exhibit more complex geometry.

A series of numerical experiments were performed to test the effectiveness of the Dubins’ type initial guess generation method for improving the convergence of the DENMRA when solving the minimum-time emergency landing problem. In all experiments, certain boundary conditions were kept fixed, including the initial speed $v_0 = 240$ m/s, the final speed $v_f = 95$ m/s, the initial path angle $\gamma_0 = 0$ deg, the final path angle $\gamma_f = 0$ deg, the initial position $x_0 = 0$ km, $y_0 = 0$ km, and the initial heading angle $\psi_0 = 0$ deg. The other boundary conditions were generated randomly for each experiment. Specifically, the airport position was sampled uniformly from a disc on the

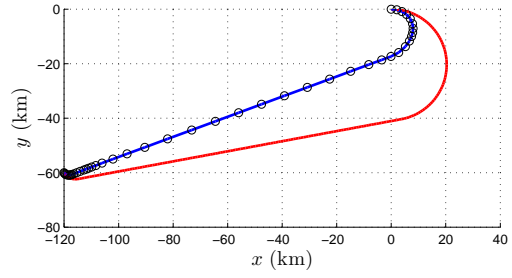
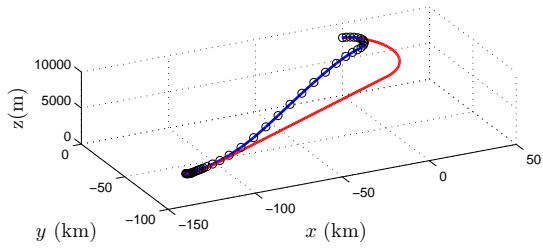


Figure 4. Trajectory comparison, case 1.

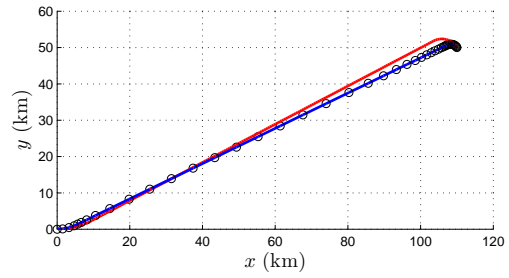
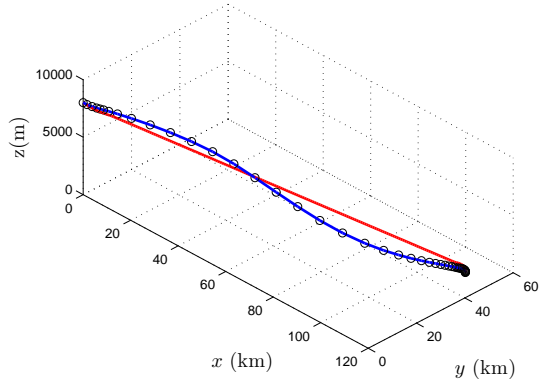


Figure 5. Trajectory comparison, case 2.

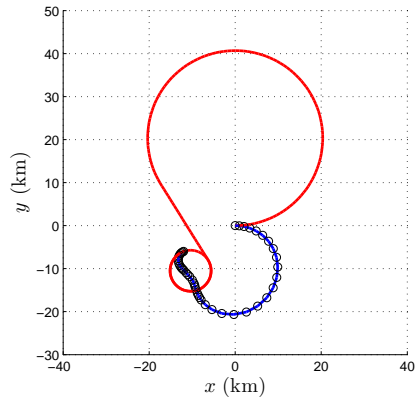
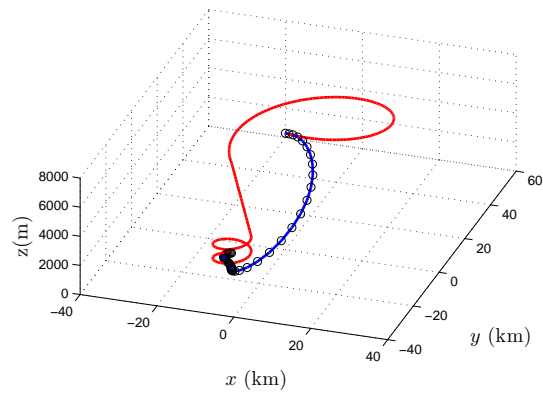


Figure 6. Trajectory comparison, case 3.

ground (zero altitude) with radius $R_{\max} = 200$ km, the runway heading being uniformly distributed in $[0, 2\pi]$, and the initial altitude being uniformly distributed between 6 km and 10 km.

In each experiment, after the boundary conditions were determined, a three-dimensional landing trajectory was generated as discussed in Sections II-IV, and was subsequently applied as an initial guess for DENMRA. As a comparison, in each experiment, an affine initial guess interpolating the boundary conditions was also used as the initial guess for DENMRA, for comparison.

The details about the boundary conditions and sampling process for the numerical experiments are shown below:

$$\begin{aligned} x_0 &= 0, & y_0 &= 0, & z_f &= 0, & \psi_0 &= 0, \\ \gamma_0 &= 0, & \gamma_f &= 0, & v_0 &= 240, & v_f &= 95, \\ z_0 &\leftarrow U([6, 10])\text{km}, & \psi_f &\leftarrow U([0, 2\pi]), & \theta &\leftarrow U([0, 2\pi]), & \varpi &\leftarrow U([0, 1]), \\ R &= R_{\max}\sqrt{\varpi}, & x_f &= x_0 + R_{\max}\cos\theta, & y_f &= y_0 + R_{\max}\sin\theta, \end{aligned}$$

where $U([a, b])$ is a random number uniformly distributed on the interval $[a, b]$, R_{\max} is the maximum cross range during the landing process, which was chosen as $R_{\max} = 200$ km in all the experiments.

A total of 500 experimental cases were performed. The statistical analysis of the results showed that DENMRA converged successfully for 49.3% of all cases when an affine initial guess was used. When the Dubins' type initial guess is used, the convergence rate climbed to 99.2%, which is an enormous improvement compared to an (uninformed) affine initial guess.

VII. Conclusion

In this paper, we introduced a simple-yet effective-way to construct an initial guesses for the numerical solution of the aircraft landing trajectory optimization problem. Numerical experiments showed that, in most cases, such a simple trajectory actually captures the salient features of the optimal solution, thus facilitating the convergence of the NLP solver when applied as an initial guess. It is expected that higher convergence rate of the NLP solver can be achieved after refining the current geometric landing path generation method so that it always returns paths that correspond to feasible trajectories for the higher fidelity model of the aircraft.

References

- ¹Zhao, Y. and Tsiotras, P., "Density Functions for Mesh Refinement in Numerical Optimal Control," *Journal of Guidance, Control, and Dynamics*, Vol. 34, No. 1, 2011, pp. 271–277.
- ²Kelley, H. J., "Flight Path Optimization with Multiple Time Scales," *AIAA Journal of Aircraft*, Vol. 8, No. 4, 1971, pp. 238–240.
- ³Calise, A. J., "Extended Energy Management Methods for Flight Performance Optimization," *AIAA Journal*, Vol. 15, No. 3, 1977, pp. 314–321.
- ⁴Burrows, J. W., "Fuel-Optimal Aircraft Trajectories with Fixed Arrival Times," *Journal of Guidance, Control, and Dynamics*, Vol. 6, No. 1, 1983, pp. 14–19.
- ⁵Chakravarty, A., "Four-Dimensional Fuel-Optimal Guidance in the Presence of Winds," *Journal of Guidance, Control, and Dynamics*, Vol. 8, No. 1, 1985, pp. 16–22.
- ⁶Grimm, W., Well, K., and Oberle, H., "Periodic Control for Minimum-Fuel Aircraft Trajectories," *Journal of Guidance, Control, and Dynamics*, Vol. 9, No. 2, 1986, pp. 169–174.
- ⁷Seywald, H., Cliff, E. M., and Well, K. H., "Range Optimal Trajectories for an Aircraft Flying in the Vertical Plane," *Journal of Guidance, Control, and Dynamics*, Vol. 17, No. 2, 1994, pp. 389–398.
- ⁸Seywald, H., "Long Flight-Time Range-Optimal Aircraft Trajectories," *Journal of Guidance, Control, and Dynamics*, Vol. 19, No. 1, 1994, pp. 242–244.
- ⁹Kato, O. and Sugiura, I., "An Interpretation of Airplane General Motion and Control as Inverse Problem," *Journal of Guidance, Control, and Dynamics*, Vol. 9, No. 2, 1986, pp. 198–204.
- ¹⁰Karelahti, J., Virtanen, K., and Öström, J., "Automated Generation of Realistic Near-Optimal Aircraft Trajectories," *Journal of Guidance, Control, and Dynamics*, Vol. 31, No. 3, 2008, pp. 674–688.

- ¹¹Lu, P. and Pierson, B. L., “Optimal Aircraft Terrain-Following Analysis and Trajectory Generation,” *Journal of Guidance, Control, and Dynamics*, Vol. 18, No. 3, 1995, pp. 555–560.
- ¹²Bulirsch, R., Montrone, F., and Pesch, H. J., “Abort Landing in the Presence of Windshear as a Minimax Optimal Control Problem, Part I: Necessary Conditions,” *Journal of Optimization Theory and Applications*, Vol. 70, No. 1, 1991, pp. 1–23.
- ¹³Bulirsch, R., Montrone, F., and Pesch, H. J., “Abort Landing in the Presence of Windshear as a Minimax Optimal Control Problem, Part II: Multiple Shooting and Homotopy,” *Journal of Optimization Theory and Applications*, Vol. 70, No. 2, 1991, pp. 223–254.
- ¹⁴Miele, A., “Optimal trajectories and guidance trajectories for aircraft flight through windshears,” *Proceedings of the 29th IEEE Conference on Decision and Control*, Vol. 2, Honolulu, HI, Dec 1990, pp. 737–746.
- ¹⁵Stryk, O. V. and Bulirsch, R., “Direct and Indirect Methods for Trajectory Optimization,” *Journal of Guidance, Control, and Dynamics*, Vol. 37, 1992, pp. 357–373.
- ¹⁶Shen, H. and Tsiotras, P., “Time-Optimal Control of Axisymmetric Rigid Spacecraft Using Two Controls,” *Journal of Guidance, Control, and Dynamics*, Vol. 22, No. 5, Sep.-Oct. 1999, pp. 682694.
- ¹⁷Gath, P. F., Well, K. H., and Mehlem, K., “Initial Guess Generation for Rocket Ascent Trajectory,” *AIAA Journal of Spacecraft and Rockets*, Vol. 29, No. 4, Jul.-Aug. 2002, pp. 515–521.
- ¹⁸Dubins, L. E., “On curves of minimal length with a constraint on average curvature, and with prescribed initial and terminal positions and tangents,” *American Journal of Mathematics*, Vol. 79, No. 3, 1957, pp. 497–516.
- ¹⁹Sussmann, H. J., “Shortest 3-dimensional path with a prescribed curvature bound,” *Proceedings of 34th IEEE Conference on Decision and Control*, New Orleans, LA, December 1995, pp. 3306–3312.
- ²⁰Chitsaz, H. and LaValle, S. M., “Time-optimal paths for a Dubins airplane,” *Proceedings of 46th IEEE Conference on Decision and Control*, New Orleans, LA, December, 12-14 2007, pp. 2379–2384.
- ²¹Sussmann, H. J. and Tang, G., “Shortest paths for the Reeds-Shepp car: a worked out example of the use of geometric techniques in nonlinear optimal control,” Research Note SYCON-91-10, Rutgers University, New Brunswick, NJ, 1991.
- ²²Bui, X.-N., Souères, P., Boissonnat, J.-D., and Laumond, J.-P., “Shortest path synthesis for Dubins non-holonomic robot,” *Proceedings of the 11th IEEE Intern. Conf. on Robotics and Automation (ICRA)*, San Diego, California, 1994.
- ²³Souères, P. and Laumond, J.-P., “Shortest path synthesis for a car-like robot,” *IEEE Transactions on Automatic Control*, Vol. 41, No. 5, 1996, pp. 672–688.
- ²⁴Zhao, Y. and Tsiotras, P., “Time-Optimal Parametrization of Geometric Paths for Fixed-Wing Aircraft,” *AIAA Infotech at Aerospace*, Atlanta, GA, April 20–22 2010, AIAA Paper 2010-3352.
- ²⁵Bakolas, E. and Tsiotras, P., “Optimal Synthesis of the asymmetric sinistral/dextral Markov-Dubins problem,” *Journal of Optimization Theory and Applications*, Vol. 150, No. 2, 2011, pp. 233–250.
- ²⁶Etkin, B., *Dynamics of Atmospheric Flight*, Dover Publications, 2005.
- ²⁷NASA, “Earth atmosphere model,” <http://www.grc.nasa.gov/WWW/K-12/airplane/atmosmet.html>, retrieved Aug, 2009.
- ²⁸Betts, J. T. and Huffman, W. P., “Mesh Refinement in Direct Transcription Methods for Optimal Control,” *Optimal Control Applications and Methods*, Vol. 19, No. 1, 1998, pp. 1–21.
- ²⁹Gill, P. E., Murray, W., and Saunders, M. A., “SNOPT: An SQP Algorithm for Large-scale Constrained Optimization,” Numerical analysis report 97-2, University of California, San Diego, La Jolla, CA, 1997.